

***Six1* controls patterning of the mouse otic vesicle**

Hidegori Ozaki¹, Kazuaki Nakamura¹, Jun-ichi Funahashi², Keiko Ikeda¹, Gen Yamada³, Hisashi Tokano⁴, Hiro-oki Okamura⁴, Ken Kitamura⁴, Shigeaki Muto⁵, Hayato Kotaki⁶, Katsuko Sudo⁶, Reiko Horai⁶, Yoichiro Iwakura⁶ and Kiyoshi Kawakami^{1,*}

¹Division of Biology, Center for Molecular Medicine, Jichi Medical School, Tochigi 329-0498, Japan

²Department of Molecular Neurobiology, Institute of Development, Aging and Cancer, Tohoku University, Sendai 980-8575, Japan

³Division of Transgenic Technology, Center for Animal Resources and Development, Kumamoto University, Kumamoto 860-0811, Japan

⁴Department of Otolaryngology, Tokyo Medical and Dental University, Tokyo 113-8519, Japan

⁵Division of Nephrology, Department of Internal Medicine, Jichi Medical School, Tochigi 329-0498, Japan

⁶Division of Cell Biology, Center for Experimental Medicine, Institute of Medical Science, University of Tokyo, Tokyo 108-8639, Japan

*Author for correspondence (e-mail: kkawakam@jichi.ac.jp)

Accepted 24 October 2003

Development 131, 551-562
Published by The Company of Biologists 2004
doi:10.1242/dev.00943

Summary

Six1 is a member of the Six family homeobox genes, which function as components of the Pax-Six-Eya-Dach gene network to control organ development. *Six1* is expressed in otic vesicles, nasal epithelia, branchial arches/pouches, nephrogenic cords, somites and a limited set of ganglia. In this study, we established *Six1*-deficient mice and found that development of the inner ear, nose, thymus, kidney and skeletal muscle was severely affected. *Six1*-deficient embryos were devoid of inner ear structures, including cochlea and vestibule, while their endolymphatic sac was enlarged. The inner ear anomaly began at around E10.5 and *Six1* was expressed in the ventral region of the otic vesicle in the wild-type embryos at this stage. In the otic vesicle of *Six1*-deficient embryos, expressions of *Otx1*, *Otx2*, *Lfng* and *Fgf3*, which were expressed ventrally in the wild-type otic vesicles, were abolished, while the expression

domains of *Dlx5*, *Hmx3*, *Dach1* and *Dach2*, which were expressed dorsally in the wild-type otic vesicles, expanded ventrally. Our results indicate that *Six1* functions as a key regulator of otic vesicle patterning at early embryogenesis and controls the expression domains of downstream otic genes responsible for respective inner ear structures. In addition, cell proliferation was reduced and apoptotic cell death was enhanced in the ventral region of the otic vesicle, suggesting the involvement of *Six1* in cell proliferation and survival. In spite of the similarity of otic phenotypes of *Six1*- and *Shh*-deficient mice, expressions of *Six1* and *Shh* were mutually independent.

Key words: *Six1*, Otic vesicle, Inner ear, Pattern formation, Cell proliferation, *Shh*, Mouse

Introduction

The Six gene family was identified as a homologue of the *Drosophila sine oculis* (*so*) and is conserved in various species (Seo et al., 1999; Kawakami et al., 2000). Six gene products are characterized by the Six domain and Six-type homeodomain, which are required for specific DNA binding activity and function as transcription factors (Kawakami et al., 1996; Spitz et al., 1998; Ohto et al., 1999; Li et al., 2002; Lagutin et al., 2003). At present, six members of the family have been identified in mammals, and all members show a spatiotemporally regulated pattern of expression during embryogenesis, suggesting their involvement in embryonic development (Seo et al., 1999; Kawakami et al., 2000). The Six gene family is known to function as a component of the Pax-Six-Eya-Dach gene network. This property was originally identified in genetic studies using *Drosophila*. Compound eye formation has been extensively examined as a model system of organ development, and the important eye-forming genes, *eyeless* (*ey*, a *Pax6* homologue), *twin of eyeless* (*toy*, another *Pax6* homologue), *sine oculis* (*so*, a Six homologue), *eyes absent* (*eya*, an Eya homologue) and *dachshund* (*dac*, a Dach

homologue), have been identified. Genetic and biochemical studies have revealed the hierarchy, cooperative relationships and physical interactions among these genes and their encoded proteins; *toy* activates *ey* (Czerny et al., 1999), and *ey* and/or *toy* activate *so* and *eya* (Halder et al., 1998; Niimi et al., 1999; Zimmerman et al., 2000), then *so* and *eya* cooperate to activate *dac* (Pignoni et al., 1997; Chen et al., 1997). In addition to such a hierarchy, reciprocal feedback loops operate to form complex regulatory gene networks (Chen et al., 1997; Pignoni et al., 1997). Of note is that the vertebrate homologues of these *Drosophila* genes, *Pax6* (Walther and Gruss, 1991), *Six3/Six6* (Oliver et al., 1995a; Toy et al., 1998), *Eya1/Eya2/Eya3* (Xu et al., 1997) and *Dach1/Dach2* (Caubit et al., 1999; Davis et al., 2001), are expressed in the developing eyes, and some of them were shown to be involved in eye development (Hill et al., 1991; Ton et al., 1991; Glaser et al., 1992; Oliver et al., 1996; Kobayashi et al., 1998; Loosli et al., 1999; Lagutin et al., 2001; Carl et al., 2002; Li et al., 2002; Lagutin et al., 2003). A similar gene network was found to control chick myogenesis, in which *Six1*, *Eya2* and *Dach2* synergistically regulate the expression of myogenic genes such as myogenin and *MyoD* (Heanue et

al., 1999). In addition, *Pax3* induces the expression of *Six1* and *Eya2* before induction of *MyoD* and myogenin expression (Ridgeway and Skerjanc, 2001). *Pax3* is involved in myogenesis also by activating *Dach2* expression and is reciprocally activated by *Dach2* (Heanue et al., 1999; Kardon et al., 2002). Furthermore, homologues of these gene families are expressed in various developing organs in a spatially and temporally overlapping manner during embryogenesis, suggesting that similar gene networks regulate the development of various organs in addition to the eye and skeletal muscles. In fact, an increasing number of loss-of-function mutations in Pax, Eya and Six genes have been reported to cause defects in various organs. *Pax2*-deficient mice show defects in eyes, ears and the urogenital system (Favor et al., 1996; Torres et al., 1996). Loss of *Eya1* in mice results in the absence or anomalies in the ear, thymus, parathyroid gland, kidney, thyroid and skeleton (Xu et al., 1999; Xu et al., 2002). For Six genes, inactivation of mouse *Six6* is associated with hypogenesis of the pituitary gland and retina (Li et al., 2002). *SIX3* mutations in humans cause holoprosencephaly, and *Six3* inactivation in mice results in a lack of anterior head structures, including eyes and nose (Wallis et al., 1999; Lagutin et al., 2003).

Six1 is expressed in otic vesicles, nasal epithelia, branchial arches/pouches, nephrogenic cords, somites and a limited set of ganglia (Oliver et al., 1995b). However, it is unknown whether or how *Six1* is involved in the development of the inner ear, nose, branchial arch/pouch-derived organs, kidney, ganglia and skeletal muscles. To address this question, we generated and analyzed the organ development of *Six1*-deficient mice. The inner ear, nose, thymus, kidney and skeletal muscles are severely affected in *Six1*-deficient mice, suggesting crucial roles for *Six1* in the development of these organs. Among these phenotypes, the defects in inner ear development in the mutant mice are intriguing because inner ears develop elaborate structures with precise disposition and orientation in normal embryogenesis. They are derived from the otic vesicle by successive transformation and compartmentalization, but it is poorly understood how the patterning of the otic vesicle is established and what are the key factors for such complex processes. Thus, this paper focused on the analysis of inner ear development and identified the essential roles of *Six1* in otic vesicle patterning.

Materials and methods

Construction of the *Six1* targeting vector

The entire coding region of the murine *Six1* gene was isolated from a 129/SvJ mouse genomic library (Stratagene, La Jolla, California) using a *Six1* cDNA (Oliver et al., 1995b) as a probe, and the exon-intron organization was determined. An *NcoI* site was generated at the initiation codon by PCR mutagenesis to allow the insertion of an in-frame enhanced green fluorescent protein (EGFP) gene. The targeting vector was constructed in pBluescript KS(+) (Stratagene) and the organization is shown in Fig. 1A. In this construct the entire coding region, including exons 1 and 2, the intervening intron and the short stretch of the 3' untranslated region of exon 2, were replaced with an EGFP fragment (*NcoI*-*SspI*, 1.0 kb) from pEGFP-N3 (Clontech, Palo Alto, California) and an *hph* cassette (*EcoRV*-*PvuII*, 2 kb) from pPGK-*hph*-*bpA* (Horai et al., 1998). The diphtheria toxin A cassette (dt) (*XhoI*-*NotI*, 1.4 kb) from pMC1DTpA (Yagi et al., 1993) was added at the 3' terminus for the

negative selection. The resulting plasmid was linearized with *SaII* at the 5' end of the insert.

ES cell screening and chimeric mouse production

The linearized targeting vector (80 µg) was electroporated (250 V, 500 µF) into 1×10^7 E14.1 ES cells (Kuhn et al., 1991) and transformants were selected with hygromycin B (230 µg/ml; Invitrogen Japan K.K., Tokyo) for 5-9 days. Homologous recombinants were screened by Southern blot hybridization. Genomic DNA from each resistant clone was digested with *NcoI*, analyzed by Southern blotting using the probes *NcoI*-*SacI*, 1.2 kb fragment upstream of 5' homology (5' probe), and *XbaI*-*EcoRI*, 2.0 kb fragment downstream of 3' homology (3' probe), to confirm the correct homologous recombination at 5' and 3' sides, respectively (Fig. 1A). Chimeric mice were produced by the aggregation method (Horai et al., 1998). Male chimeras were bred with C57BL/6 female mice to check germline transmission. Heterozygous mice were intercrossed to produce *Six1*-deficient mice. Genotyping was carried out by Southern blot analysis (Fig. 1B) or PCR (data not shown) in combination with morphological analyses. In the PCR analysis, the targeted allele was detected with primers WtmSix1F (GCG CCC GGG CCC GTG CGC CCC) and KOmSix1R (TGC CCC AGG ATG TTG CCG TCC), and the wild-type allele with primers WtmSix1F and WtmSix1R (GCT TTC AGC CAC AGC TGC TGC).

In this study, *Shh* mutant mice with a targeted deletion of exon 2 of the gene were also used (Chiang et al., 1996) (kindly supplied by C. Chiang and C. C. Hui).

Mice were kept under specific pathogen-free conditions in environmentally controlled clean rooms at the Center for Experimental Medicine, Jichi Medical School, and at the Laboratory Animal Research Center, Institute of Medical Science, University of Tokyo. All mice used in this study were sacrificed by cervical translocation or anesthetization with diethyl ether. The experiments were conducted according to the institutional ethical guidelines for animal experiments and safety guidelines for gene manipulation experiments.

Histological examinations

Embryos and neonates were fixed in 10% formalin or 4% PFA in PBS, embedded in paraffin wax and then cut into 5-µm thick serial sections. De-waxed sections were stained with hematoxylin and eosin as described previously (Ozaki et al., 2001). Alcian Blue/Alizarin Red staining of neonatal skeletons was performed as described previously (Wallin et al., 1994).

RNA in situ hybridization

In situ hybridization was performed using digoxigenin (DIG)-labeled antisense riboprobes as described previously (Xu and Wilkinson, 1998). *Eya1* riboprobe was synthesized from a 528 bp *HindIII* fragment of pHM6Eya1 (Ohto et al., 1999) subcloned into pBluescript KS(+). *Six4* riboprobe was synthesized from a 630 bp *PstI* fragment (ntd 1545-2175 of *Six4* SM type cDNA) subcloned into pBluescript KS(+). The following cDNAs were also used for in situ hybridization probes: *Six1* (Oliver et al., 1995b), *Otx1* and *Otx2* (Matsuo et al., 1995), *Fgf3* (Wilkinson et al., 1988), *Lfng* (Morsli et al., 1998), *Dlx5* (Miyama et al., 1999), *Dach1* (Caubit et al., 1999), *Dach2* (Davis et al., 2001), *Pax2* (Nishinakamura et al., 2001), *Bmp4* (a kind gift from N. Ueno), *Hmx3* (Wang et al., 1998), *Shh* (Uruse et al., 1996), *Ptch* (Goodrich et al., 1996), *Gli1* (Hui et al., 1994), *Wnt2b* (Riccomagno et al., 2002).

TUNEL analysis

For terminal deoxynucleotidyl transferase-mediated dUDP nick-end labeling (TUNEL), embryos were fixed in 4% PFA in PBS, embedded in OCT compound, and frozen and sectioned into serial cryosections. Apoptotic cells were detected with the In Situ Cell Death Detection Kit, POD (Roche Diagnostics Mannheim, Germany). Briefly,

fragmented DNA in apoptotic cells was end-labeled with fluorescein and the labeled DNA was detected with anti-fluorescein antibody conjugated with peroxidase and a chromogenic substrate.

BrdU incorporation

Pregnant female mice of gestation day 10.5 and 11.5 were intraperitoneally injected with 100 mg 5-bromo-2'-deoxyuridine (BrdU) per kg body weight. Embryos were collected 1.5 hours later and processed for preparation of 8- μ m thick paraffin sections as described above. De-waxed serial sections crossing otic vesicles were treated with 2 N HCl/0.5% Triton X-100 in PBS for 30 minutes at room temperature and rinsed with 0.1 M borate buffer (pH 8.5), followed by incubation in 0.6% H₂O₂ in PBS for 30 minutes at room temperature. Subsequently, the sections were incubated overnight in peroxidase-labeled anti-BrdU (Roche) at 4°C. After washing, sections were stained in 0.4 mg/ml diaminobenzidine, 0.68 mg/ml imidazole, 0.01% H₂O₂, and 50 mM Tris-HCl (pH 7.4).

Paint-fill analysis

Paint-fill was performed as described previously (Bissonnette and Fekete, 1996). In brief, embryos were fixed in Bodian's fixative, dehydrated through graded ethanol solutions, then cleared in methyl salicylate and injected into the lumen of the membranous labyrinth with white paint diluted 1 to 100 in methyl salicylate.

ABR threshold measurements

The auditory evoked response was recorded with stainless steel needle electrodes inserted subcutaneously into the vertex (active), left and right of the retro-audicular regions (inactive) and the opposite thigh (ground). The stimulus sound in peak equivalent sound pressure level (peSPL) of a tone pips of 0.1 millisecond slopes, 1 millisecond duration, 70 millisecond repeat interval with 5.6, 8.0, 12.0, 18.0, 24.0, 32.0 kHz frequencies was given by free field in an electrically shielded room. A tweeter (PT-R111, Pioneer) was placed 10 cm in front of the external acoustic foramen. The stimulus sound pressure was corrected by a Bruel & Kjaer-type 2636 noise meter. A microcomputer (ER-2104, GE Marquet) was used to analyze the response. Auditory

thresholds were obtained for each stimulus by varying at 10 dB steps up and down to identify the lowest level at which an auditory brain response (ABR) pattern could be recognized. These experiments were conducted in five wild-type and six heterozygous mice at 5 to 6 weeks of age.

Results

Generation of *Six1*-deficient mice

To explore the developmental roles of *Six1*, we inactivated *Six1* in ES cells by replacing the entire coding region with EGFP gene (Fig. 1A). Two independent ES clones were confirmed as homologous recombinants (data not shown), and both of them gave germline chimeric mice. These chimeric mice were crossed with C57BL/6 to obtain F1 heterozygous mutant mice. Heterozygotes appeared normal in appearance and grew up to adulthood as wild type (data not shown). The concentrations of Na⁺, K⁺, Cl⁻, Ca²⁺, Mg²⁺, inorganic phosphate, urea nitrogen, creatinine, albumin and uric acid in serum and urine were measured with an auto-analyzer, and we observed no significant difference in the concentrations of all these parameters between the wild-type and heterozygous mutant mice (data not shown). We also performed ABR testing for hearing impairment in the heterozygous mutant mice. The ABR thresholds were 25.0 \pm 5.3, 14.0 \pm 5.2, 14.0 \pm 5.2, 11.0 \pm 3.2, 10.0 \pm 0.0 and 14.0 \pm 5.2 dBpeSPL for the wild-type mice and 23.3 \pm 4.9, 15.0 \pm 5.2, 10.8 \pm 2.9, 10.0 \pm 0.0, 10.8 \pm 2.9 and 14.2 \pm 5.1 dBpeSPL for the heterozygotes at frequencies of 5.6, 8.0, 12.0, 18.0, 24.0 and 32.0 kHz, respectively, and there were no significant differences in these values between the wild-type and heterozygous mutant mice.

Homozygous mutants were born at Mendelian frequency and showed few body movements but were apnoeic and died immediately after birth. They had micrognathia, and the eyelids were sometimes open (data not shown). No *Six1* mRNA was detected in homozygotes (Fig. 1C), confirming that the entire coding region of *Six1* was replaced by EGFP gene in this mutant. In the following analyses, we used neonates and embryos from F1 heterozygous matings.

Defects in ears, nose, thymus, kidneys and skeletal muscles of *Six1*-deficient neonates

Dissection analyses and hematoxylin and eosin (H-E) staining of sections of the neonates revealed defects in the ears, nose, thymus, kidneys and skeletal muscles in

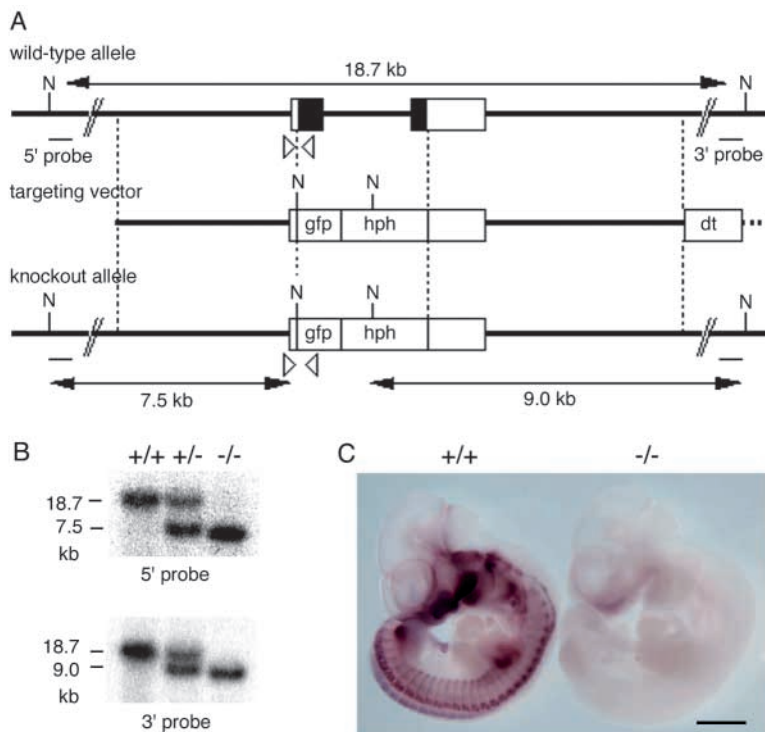


Fig. 1. Generation of *Six1*-deficient mice. (A) Targeting strategy of *Six1*. The *Six1* gene consists of two exons (indicated by boxes), and the coding regions are marked in black. The entire coding regions were replaced with the EGFP gene (*gfp*) and the *hygromycin-B-phosphotransferase* gene (*hph*). Open arrowheads indicate the positions of PCR primers for genotyping. (B) Southern blot analyses of wild-type (+/+), heterozygous (+/-), and homozygous (-/-) mutant neonates. Tail DNA was digested with *NcoI* and hybridized to 5' probe (upper panel) and 3' probe (lower panel). The size of each band is indicated on the left side. (C) In situ hybridization to *Six1* in E10.5 wild-type and homozygous embryos. Absence of *Six1* mRNA was confirmed in the *Six1*-deficient embryo. *dt*, diphtheria toxin A gene; *N*, *NcoI* site. Scale bar: 1 mm.

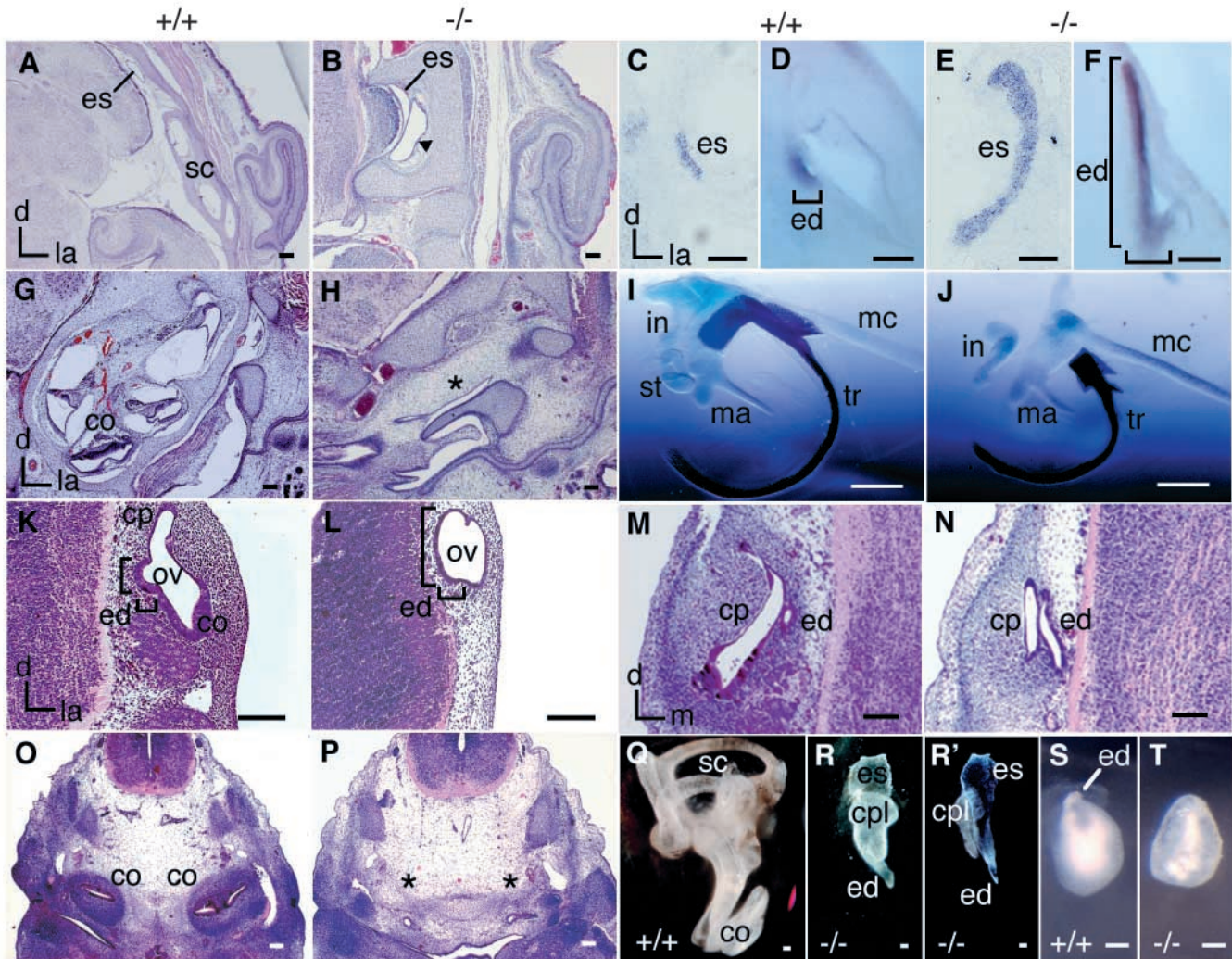


Fig. 2. Defects in the inner and middle ear in *Six1*-deficient mice. (A,B) Transverse sections at the level of the pinna of the neonates. The semicircular canals and the endolymphatic sac are irregularly formed in the *Six1*^{-/-} neonates. The semicircular canals and the common crus are fused, forming a large cavity (B, arrowhead). (C-F) *Wnt2b* expression analysis by in situ hybridization. Expansion of the *Wnt2b* expression domain in the *Six1*^{-/-} embryos (E,F) compared with wild type (C,D) indicates that the enlarged region is the endolymphatic sac at E17.5 (E) and endolymphatic duct at E11.5 (F). In F, *Wnt2b* was expressed in the medial half of the otic vesicle, which corresponds to the enlarged endolymphatic duct as depicted in L (otic vesicle shown in F was flattened during the hybridization process). (G,H) Transverse sections at the cochlea level show complete loss of the cochlea in *Six1*^{-/-} neonates (asterisk). (I,J) Alcian blue/Alizarin red staining of neonatal skeletons revealed malformations of ossicles. (K,L) Transverse sections of wild-type (K) and *Six1*^{-/-} (L) embryos at E11.5. The cochlear region does not extend ventrally and the endolymphatic duct is dilated in *Six1*^{-/-} embryos. (M-P) Transverse sections of wild-type (M,O) and *Six1*^{-/-} (N,P) embryos at E12.5. The endolymphatic duct and canal plate are formed, but the morphology is abnormal in the *Six1*^{-/-} embryo (N). The cochlea is completely absent in *Six1*^{-/-} embryos (P, asterisks). (Q-T) Lateral views of the paint-filled inner ear of wild-type (Q) and *Six1*^{-/-} (R) E18.5 embryos and otic vesicles of wild-type (S) and *Six1*^{-/-} (T) E10.5 embryos. (R') Posterior view of the same inner ear as (R). Relative positions are aligned between wild type and *Six1*^{-/-}. The two ventrally protruding structures observed in (R and R') are the ventral ends of residual cavities of the canal plate-like structure and the endolymphatic duct. More than five *Six1*^{-/-} neonates or embryos at each stage were analyzed, and virtually the same results were obtained. co, cochlea; cp, canal plate; cpl, canal plate-like structure; d, dorsal; ed, endolymphatic duct; es, endolymphatic sac; in, incus; la, lateral; m, medial; ma, malleus; mc, Meckel's cartilage; ov, otic vesicle; sc, semicircular canals; st, stapes; tr, tympanic ring. Scale bars: 100 μ m.

the *Six1*-deficient mice. In the inner ear, the dorsalmost parts of semicircular canals and common crus remained as a common fused space. The endolymphatic sac was present but was irregularly larger in size than that of wild-type littermates (Fig. 2A,B). The enlargement was confirmed by comparing the diameter of the paint-filled endolymphatic sacs of the *Six1*-deficient and the wild-type embryos (data not shown). The

expansion of the expression domain of *Wnt2b*, an expression marker for the endolymphatic sac and duct, also supports the enlargement of the endolymphatic sac (Fig. 2C,E). Other parts of the inner ear were completely absent, including the cochlea, vestibule and accompanying vestibulo-acoustic ganglia (Fig. 2G,H, data not shown). These structural defects were also demonstrated by paint-fill analyses (Fig. 2Q,R,R'). Because *Six1*

expression was evident in the branchial arch and periotic mesenchymes (Fig. 1C, Fig. 4C), we examined the middle ear defects in the *Six1*-deficient neonates and found malformations of the malleus and the incus and the absence of the stapes (Fig. 2I,J). In the nose, *Six1*-deficient mice manifested a hollowed nasal region with traces of nasal bleeding (data not shown). A pair of mere simple, rounded nostrils was present with no nasal epithelium, by contrast to the well-branched cavities with thick layers of nasal epithelia in the wild-type littermates (Fig. 3A,B). Both nasal cavities did not connect with the oral cavity or the nasopharynx, and the vomeronasal organs were absent in *Six1*-deficient mice (data not shown). The surrounding ossified region was abnormally enlarged (Fig. 3B), as observed in the inner ear (Fig. 2B,H). *Six1*-deficient mice also lacked a thymus (Fig. 3C,D). Kidneys were severely affected to variable degrees (Fig. 3E,F). Small kidneys with normal structure were found in mild cases (data not shown), while both kidneys were absent in extreme cases, although the ureters were always formed but were occasionally shorter (Fig. 3F). We also found markedly reduced skeletal muscle mass of the trunk, limbs, diaphragm and tongue (Fig. 3G,H, data not shown). The thymus, kidney, ear, nose and skeletal muscle defects are consistent with the *Six1*-deficient mice with different targeting strategy (Laclef et al., 2003a; Laclef et al., 2003b; Xu et al., 2003). These affected organs correlated well with the expression sites of *Six1* during development, such as otic vesicles, nasal pits, branchial arches/pouches, nephrogenic cords and somites (Oliver et al., 1995b). These results indicate that *Six1* is required for the formation of the ear, nose, thymus, kidneys and skeletal muscles.

Defects in inner ear appear at mid-gestation in *Six1*-deficient embryos

To determine the developmental stages at which the inner ear defects start to appear, *Six1*-deficient mice of several embryonic stages were sectioned and analyzed by H-E staining. At E9.5, otic vesicles were morphologically normal in *Six1*-deficient embryos, but the vestibulo-acoustic ganglia were missing (data not shown). At E10.5 and E11.5, the otic vesicles began to compartmentalize into saccular and utricular regions. The saccular region extended to the ventral side as a thin bulge in the wild type (Fig. 2K). By contrast, the extension of the saccular region to the ventral side did not occur in *Six1*-deficient embryos (Fig. 2L). The endolymphatic duct was observed as a thin outpocketing from the medial side of the otic vesicle in wild-type embryos, while the endolymphatic duct was observed as a large swelling in *Six1*-deficient embryos (Fig. 2K,L). The thin outpocketing and the large swelling region coincided with the expression domain of *Wnt2b* (Fig. 2D,F). We also used paint-fill analyses to compare otic vesicle structures at E10.5 with those of the wild type and confirmed the absence of the thin outpocketing and the dilatation of the endolymphatic duct in *Six1*-deficient otic vesicles (Fig. 2S,T, data not shown). At E12.5, the main structures of the inner ear (cochlea, saccule, utricle, endolymphatic duct and canal plates, from which three semicircular canals and common crus are formed) were distinguishable in the wild type (Fig. 2M,O, data not shown). By contrast, the dorsal extremity of the semicircular canals and common crus was observed as a fused cavity, and abnormally large endolymphatic duct was present (Fig. 2N), while other parts were completely absent in *Six1*-deficient embryos (Fig. 2P, data not shown).

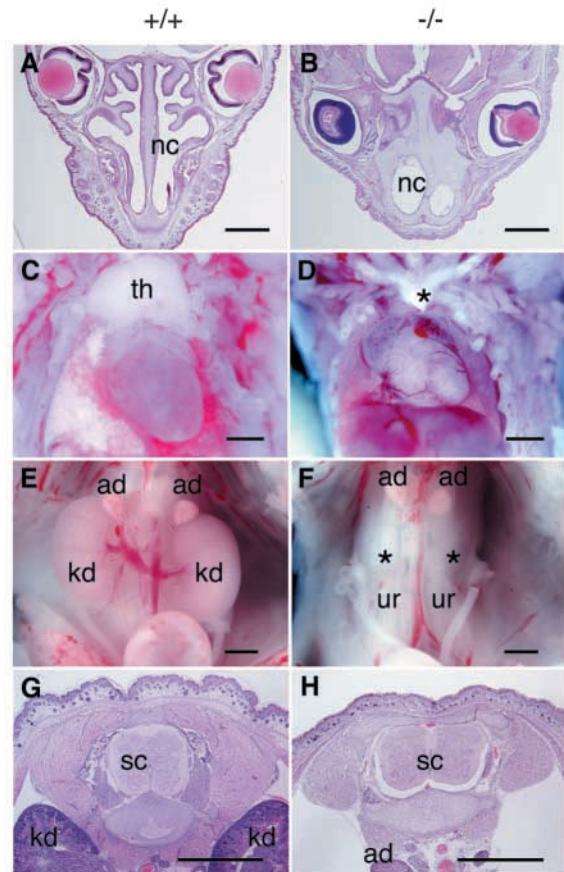


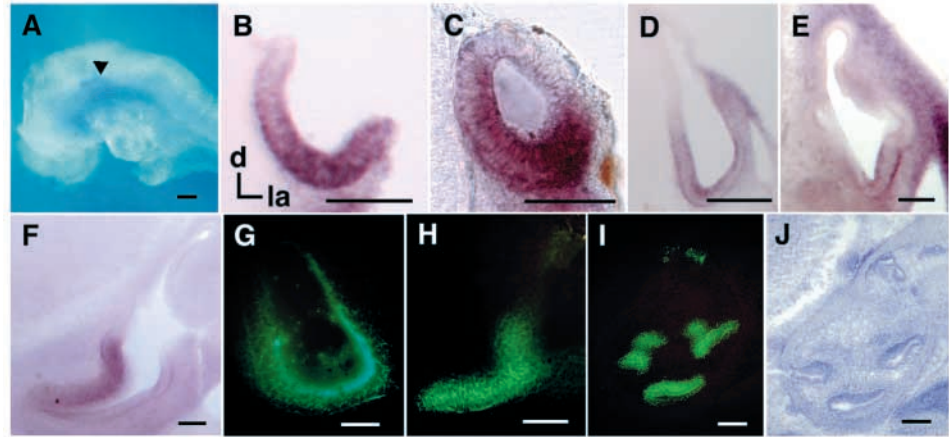
Fig. 3. Defects in the formation of the nose, thymus, kidney and skeletal muscles. Histological analyses of the wild-type (A,C,E,G) and the *Six1*^{-/-} (B,D,F,H) neonates. (A,B) Transverse sections of the nasal region. Nasal cavities form complex, branched structures with nasal epithelia in the wild type (A), and a pair of simple round cavities with no nasal epithelia is seen in the *Six1*^{-/-} neonates (B). (C,D) The thymus is prominent anterior to the heart in the wild type (C) but completely absent in the *Six1*^{-/-} neonate (D, asterisk). (E,F) Kidney defects in *Six1*^{-/-} mice. Note the bilateral renal aplasia (F, asterisks). (G,H) Abdominal transverse sections. Note severe reduction of skeletal muscle mass in *Six1*^{-/-} neonates (H). More than five pairs of wild-type and *Six1*^{-/-} neonates were analyzed and virtually the same results obtained except for the kidney (see text). ad, adrenal gland; kd, kidney; nc, nasal cavity; sc, spinal cord; th, thymus; ur, ureter. Scale bars: 1 mm.

In summary, the development of the inner ear was defective at mid-gestation around E10.5-12.5.

Expression of *Six1* in the developing inner ear

To gain insight into the function of *Six1* during inner ear development, we first examined the expression pattern of *Six1* by in situ hybridization in the wild type (Fig. 4A-F) and GFP fluorescence in heterozygous embryos (Fig. 4G-I). *Six1* mRNA was first detected in the otic placode and the surrounding surface ectoderm at E8.5 (Fig. 4A). *Six1* expression became prominent at the invaginating otic pit and the nascent otic vesicle at E9.5 (Fig. 4B,C), consistent with previous observations (Oliver et al., 1995b). Notably, the expression level was considerably lower in the dorsalmost region than in the other region of the otic vesicle (Fig. 4C). At E10.5, *Six1*

Fig. 4. *Six1* expression pattern during inner ear development detected by in situ hybridization in the wild type (A-F) and by GFP luminescence in the heterozygotes (G-I) viewed laterally (A) and in transverse sections (B-I). (A) At E8.5, *Six1* is weakly expressed in the otic placode (arrowhead) and the surrounding surface ectoderm. (B) At E9.5, *Six1* is expressed in the invaginating otic pit and (C) in the whole region of the otic vesicle except the dorsalmost region. (D,G) At E10.5, *Six1* is expressed in the ventral half of the otic vesicle. (E) At E11.5 and (F,H) E12.5, *Six1* is expressed exclusively in the cochlea. (I) Expression of *Six1* in the cochlea is maintained at E14.5 embryos. (J) A bright field image of the section in (I) stained with hematoxylin and eosin. More than three embryos at each stage were analyzed and virtually the same results obtained. d, dorsal; la, lateral. Scale bars: 100 μ m.



expression was limited to the ventral half of the otic vesicle (Fig. 4D,G). Subsequently, the expression domain of *Six1* became gradually restricted to the cochlear region at E11.5 (Fig. 4E) and E12.5 (Fig. 4F,H). At later stages, *Six1* transcripts were detected exclusively in the cochlea at E14.5 (Fig. 4I), and the expression of *Six1* in the cochlear duct persisted in the neonate (data not shown).

***Six1* is required for correct patterning of the otic vesicle**

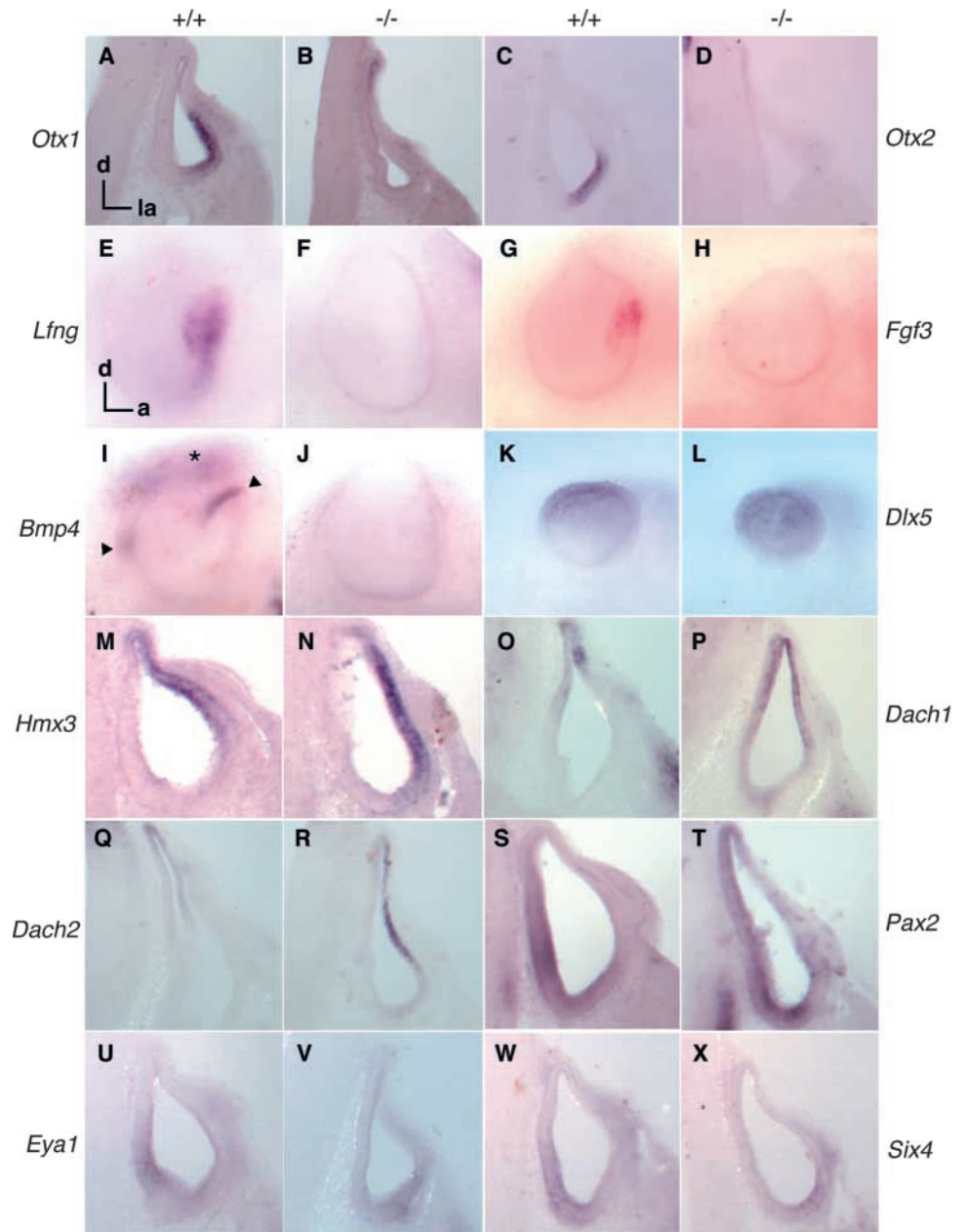
The morphological defects in *Six1*-deficient mice were not restricted to the cochlea but extended to all regions of the inner ear except the dorsal extremity of the semicircular canals (Fig. 2). The missing ventral structures of the mutant mouse inner ear appeared to be related to the expression domain of *Six1* in the ventral otic vesicle at E9.5-10.5 (Fig. 4C,D). The absence of cochlea and vestibule and the enlargement of the endolymphatic sac prompted us to examine the following three possibilities: that the specification along the dorsoventral axis within the otic vesicle is altered in *Six1*-deficient embryos, that the cells within the ventral region of the *Six1*-deficient otic vesicle undergo enhanced apoptotic cell death, and that the cells within the ventral region of the *Six1*-deficient otic vesicle proliferate at a lower rate than those of the wild type. We assessed the first possibility by comparing the expression pattern of genes differentially expressed within the otic vesicle at E9.5-10.5. The ventralmost cells of the otic vesicle are marked by the co-expression of *Otx1* and *Otx2* (Morsli et al., 1999). *Otx1* and *Otx2* were not expressed in the *Six1*-deficient otic vesicle, by contrast to the wild type, although an ectopic faint expression of *Otx1* was reproducibly detected in the dorsalmost region (Fig. 5A-D). *Lunatic Fringe* (*Lfng*), a component of the Notch signaling pathway, is known as a molecular marker for inner ear sensory structures (Morsli et al., 1998). *Lfng* was expressed in the rostroventral region in the wild type (Fig. 5E), but no such expression was noted in the *Six1*-deficient otic vesicle (Fig. 5F). *Fgf3*, which is required for normal morphogenesis of the inner ear (Mansour et al., 1993), was expressed in the rostroventral region of the wild-type otic vesicle as *Lfng* (Fig. 5G), while the expression of *Fgf3* was absent in the *Six1*-deficient otic vesicle (Fig. 5H). *Bmp4* is an

early marker for the superior, lateral and posterior cristae. It was expressed in the restricted regions of the otic vesicle in the wild type (Fig. 5I), but no such expression was noted in *Six1*-deficient mice (Fig. 5J).

The dorsal side of the otic vesicle gives rise to the semicircular canals and endolymphatic duct/sac and is well marked by the expression of *Dlx5*, which is required for the normal development of the semicircular canals and endolymphatic duct/sac (Fig. 5K) (Acampora et al., 1999; Depew et al., 1999). In *Six1*-deficient embryos, the expression domain of *Dlx5* expanded to the entire otic vesicle (Fig. 5L). The expression domains of *Hmx2* and *Hmx3*, both of which are required for the formation of the vestibular structures (Wang et al., 1998; Wang et al., 2001), expanded ventrally from the dorsolateral side in the *Six1*-deficient otic vesicle (Fig. 5M,N, data not shown). *Dach1* is a member of the Dach family genes, which constitute the Pax-Six-Eya-Dach gene network. It was also expressed at the dorsal edge of the otic vesicle in the wild-type embryos (Fig. 5O). *Dach1* expression expanded ventrally along the medial and lateral sides almost down to the ventral end in *Six1*-deficient embryos (Fig. 5P). *Dach2*, another member of Dach family genes, was expressed mainly in the dorsal end of the otic vesicle in wild-type embryos, but *Dach2* expression domain was expanded ventrally along the lateral side of the otic vesicles (Fig. 5Q,R).

We also examined the expression pattern of *Pax2*, *Eya1* and *Six4* to clarify whether the expression of these genes is dependent on *Six1*. These genes are components of the Pax-Six-Eya-Dach gene network and are co-expressed in the otic vesicle. *Pax2* was expressed in the medial side of the otic vesicle of the wild-type and *Six1*-deficient embryos (Fig. 5S,T). *Eya1* expression in the ventral side of the wild-type otic vesicle was maintained in the *Six1*-deficient otic vesicle (Fig. 5U,V). *Six4* was expressed in the ventral side of the otic vesicle in wild-type embryos, and this expression pattern was almost the same in the *Six1*-deficient embryo (Fig. 5W,X). However, the most abundantly expressed regions of *Eya1* and *Six4* appeared slightly shifted from the ventromedial (wild-type) to the ventrolateral (*Six1*-deficient) side of the otic vesicle. These results suggest that the expression of *Pax2*, *Eya1* and *Six4* in the otic vesicle is not dependent on *Six1*.

Fig. 5. *Six1* specifies the expression domains of differentially expressed genes in the otic vesicle. Transverse section or whole-mount view of the otic vesicle of in situ hybridized wild type (A,C,E,G,I,K,M,O,Q,S,U,W) and *Six1*^{-/-} embryos (B,D,F,H,J,L,N,P,R,T,V,X) of E10.5 (A-J,M-X) and E9.5 (K,L). (A,B) No *Otx1* expression in the *Six1*^{-/-} otic vesicle except for ectopic faint expression at the dorsal end. (C,D) Absence of *Otx2* transcripts in the *Six1*^{-/-} otic vesicle. (E,F) *Lfng* is expressed in the rostroventral region of the otic vesicle in the wild-type embryo but not in the *Six1*^{-/-} embryo. (G,H) *Fgf3* expression in the rostroventral region of the otic vesicle in the wild type is lost in the *Six1*^{-/-} embryo. (I,J) *Bmp4* expression in the wild-type otic vesicle (arrowheads) is lost in the *Six1*^{-/-} otic vesicle. Staining in the ectoderm over the dorsal region of the otic vesicle (asterisk) has also disappeared. (K,L) *Dlx5* is expressed dorsally in the wild type but in the whole region of the otic vesicle in the *Six1*^{-/-} embryo. (M,N) *Hmx3* expression domain is located only in the dorsolateral region in the wild type but is expanded ventrally in the *Six1*^{-/-} embryo. (O,P) *Dach1* expression is restricted to the dorsalmost region in the wild type, but the expression domain extends ventrally in the *Six1*^{-/-} otic vesicle. Signals in the neighboring mesenchyme are also observed in the lower right side of the otic vesicle. (Q,R) *Dach2* is expressed at the dorsal end of the otic vesicle in the wild type, but the expression domain of *Dach2* is expanded ventrally along the lateral side in *Six1*^{-/-}. (S,T) *Pax2* is expressed in medial and ventral sides of the otic vesicle of both wild-type and *Six1*^{-/-} embryos. (U,V) *Eya1* is expressed in the ventral side of the wild-type and the *Six1*^{-/-} otic vesicle. (W,X) *Six4* expression in the ventral side of the otic vesicle is maintained in the *Six1*^{-/-} embryo. More than three pairs of wild-type and *Six1*^{-/-} embryos were analyzed and virtually the same results obtained. A-D and M-X: top, dorsal side (d); right, lateral side (la). E-L: top, dorsal side (d); right, anterior side (a).

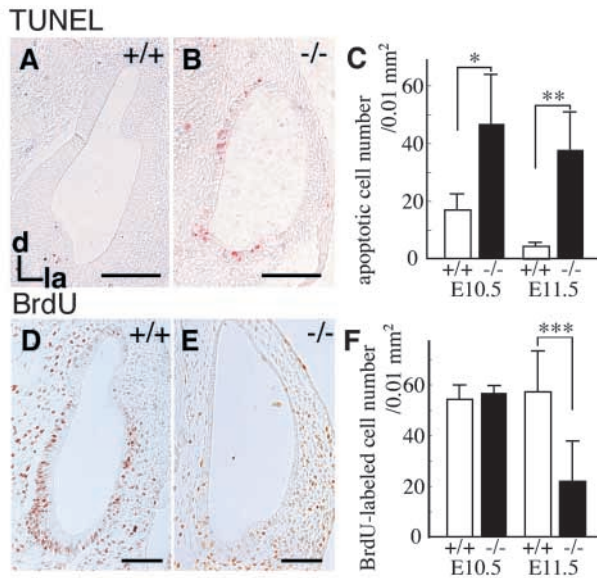


In conclusion, loss of *Six1* expression leads to marked changes in the expression domains of many genes in the otic vesicle, suggesting that the first possibility listed above is the case: i.e. the specification along the dorsoventral axis within the otic vesicle is altered in *Six1*-deficient embryos. Next, we assessed the second and third possibilities by TUNEL method and BrdU incorporation.

Enhanced apoptosis and reduced cell proliferation in the ventral otic vesicle

We examined whether enhanced apoptotic cell death or reduced cell proliferation within the ventral region of the otic

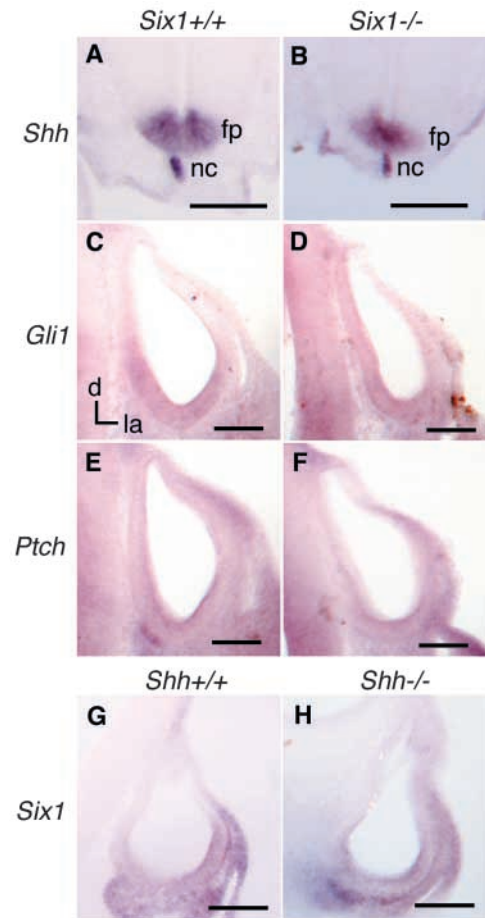
vesicle contributes to the inner ear phenotype. TUNEL method was used to detect apoptotic cells in the otic vesicle at E10.5 and E11.5, just before the extensive morphological changes. Several apoptotic cells were detected in the wild type, while enhanced apoptotic cell death was observed in the ventral and medial sides of the otic vesicles of *Six1*-deficient embryos at E11.5 (Fig. 6A,B). Statistical analysis revealed significant augmentation of apoptosis at E10.5 and E11.5 (Fig. 6C). We also examined BrdU incorporation in the otic vesicle at the same developmental stages. In the wild type and in the *Six1*-deficient embryos at E11.5, BrdU incorporation was abundant in the ventral region of the otic vesicle (Fig. 6D). By contrast,



the incorporation was profoundly reduced in the ventral side of the otic vesicles of *Six1*-deficient embryos at E11.5 (Fig. 6E). A significant decrease in the number of BrdU-incorporated cells was observed at E11.5 but not at E10.5 (Fig. 6F). The reduced cell proliferation observed in *Six1*-deficient otic vesicles may be in line with the roles of *Six1* in cell cycle control (Ford et al., 1998). These results suggest that the lack of ventral structures of the inner ear in the *Six1*-deficient mice is partly due to enhanced apoptosis and reduced cell proliferation, as well as altered patterning of the otic vesicle.

Sonic hedgehog (Shh) signaling pathway is independent of *Six1*

We noticed that the inner ear phenotype of *Six1*-deficient mice is similar to that of *Shh*-deficient mice, which is characterized by the absence of the cochlear duct and vestibulocochlear ganglia, ventral expansion of the expression domains of *Dlx5*, loss of the expression domain of *Otx2*, and ventral restriction



of *Otx1* expression (Riccomagno et al., 2002). The similarity of the phenotypes could be explained by the assumption that the Shh signaling pathway is dependent on *Six1* expression or vice versa. To test this possibility, we first examined the expression of *Shh* and the Shh-inducible genes, *Ptch* and *Gli1* in *Six1*-deficient embryos. *Shh* was expressed in the notochord and the floor plate near the otic vesicles in the wild type (Fig. 7A), and this expression pattern was virtually unchanged in *Six1*-deficient embryos (Fig. 7B). *Ptch* and *Gli1* were expressed in the otic vesicle and periotic mesenchyme in the wild-type embryo, and these expression patterns were similar in *Six1*-deficient embryos (Fig. 7C-F). Next, we examined *Six1* expression in *Shh*-deficient embryos (Chiang et al., 1996). *Six1* expression was abundant in the ventral region of the otic vesicles in *Shh*-deficient embryos, as observed in the wild type (Fig. 7G,H). These results indicate that the Shh signaling pathway is independent of *Six1* and that the expression of *Six1* in the otic vesicle is also independent of the Shh signaling pathway.

of *Otx1* expression (Riccomagno et al., 2002). The similarity of the phenotypes could be explained by the assumption that the Shh signaling pathway is dependent on *Six1* expression or vice versa. To test this possibility, we first examined the expression of *Shh* and the Shh-inducible genes, *Ptch* and *Gli1* in *Six1*-deficient embryos. *Shh* was expressed in the notochord and the floor plate near the otic vesicles in the wild type (Fig. 7A), and this expression pattern was virtually unchanged in *Six1*-deficient embryos (Fig. 7B). *Ptch* and *Gli1* were expressed in the otic vesicle and periotic mesenchyme in the wild-type embryo, and these expression patterns were similar in *Six1*-deficient embryos (Fig. 7C-F). Next, we examined *Six1* expression in *Shh*-deficient embryos (Chiang et al., 1996). *Six1* expression was abundant in the ventral region of the otic vesicles in *Shh*-deficient embryos, as observed in the wild type (Fig. 7G,H). These results indicate that the Shh signaling pathway is independent of *Six1* and that the expression of *Six1* in the otic vesicle is also independent of the Shh signaling pathway.

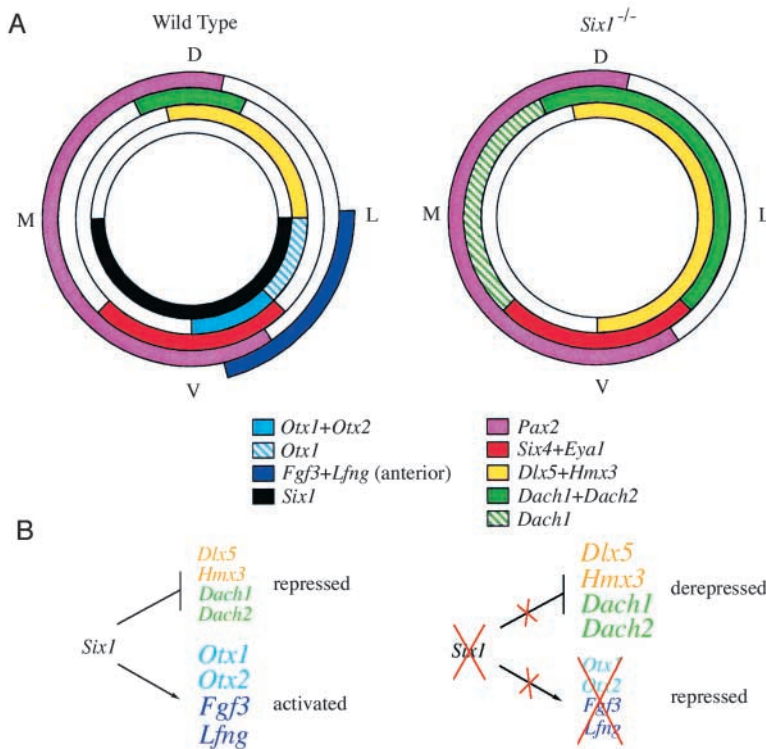


Fig. 8. (A) Schematic representation of expression of genes in otic vesicles of the wild-type (left) and *Six1*^{-/-} mice (right) at E10.5. In the otic vesicle of the wild-type, otic genes are expressed in the specified regions represented in different colors. In the wild-type otic vesicle, *Six1* is expressed in the ventral half of the otic vesicle. In the otic vesicle of *Six1*^{-/-}, the expression domains of *Dlx5*, *Hmx3*, *Dach1* and *Dach2* are expanded ventrally, and the expressions of the ventral marker genes (*Otx1*, *Otx2*, *Fgf3* and *Lfng*) are lacking due to the absence of *Six1*.

(B) Regulation of gene expression by *Six1* in the ventral otic vesicle. *Six1* activates the expression of ventral marker genes, *Otx1*, *Otx2*, *Lfng* and *Fgf3*, but represses dorsal marker genes, *Dlx5*, *Hmx3*, *Dach1* and *Dach2*, and contributes to the patterning of the otic vesicle. D, dorsal; L, lateral; M, medial; V, ventral.

directly by *Six1*, it is concluded that *Six1* plays a key role in establishing otic vesicle patterning.

In addition to the patterning of the otic vesicle along the dorsoventral axis, *Six1* may play roles in the otic vesicle patterning along the anteroposterior and/or mediolateral axes, because anteroposteriorly and/or mediolaterally asymmetrical expression patterns of *Otx1*, *Otx2*, *Lfng*, *Fgf3* and *Bmp4* were also affected (Fig. 5). For these issues, further histological examinations and analyses of molecular marker expression will be required.

Furthermore, our results showed a marked reduction of cell proliferation and enhanced apoptosis in the ventral otic vesicle in *Six1*-deficient embryos (Fig. 6). This may contribute to the inner ear phenotype lacking most of the ventral structures. Thus, *Six1* controls inner ear development by regulating cell death and proliferation as well as by establishing otic vesicle patterning.

Phenotypic similarity of the inner ear compared with *Shh*-deficient mice

Previous and present studies indicated that specification of the cochlea is dependent on *Shh* signaling and that perturbation of otic vesicle patterning in *Shh*-deficient mice (Riccomagno et al., 2002) is similar to that of *Six1*-deficient mice. Considering these phenotypic similarities of inner ear formation between *Six1*- and *Shh*-deficient mice, we assumed a genetic interaction between *Six1* and *Shh*. However, the expression patterns of *Shh*, *Gli1* and *Ptch* in *Six1*-deficient mice and that of *Six1* in *Shh*-deficient mice (Chiang et al., 1996) indicate that the expressions of *Shh*, *Gli1* and *Ptch* are not dependent on *Six1*, and that the expression of *Six1* is not dependent on the *Shh* signaling pathway in and around the otic vesicle at E10.5 (Fig. 7). Another possible mode of genetic interaction is through functional cooperation between *Six1* and the components of *Shh* signaling cascades. *Shh* protein is emanated from the notochord and/or the floor plate, probably giving a gradient of *Shh* across the otic vesicle with a high concentration in the ventral side and a low concentration in the dorsal side. This *Shh* gradient would enhance putative collaborative interaction between downstream components of *Shh* signaling cascades and *Six1* in the ventral otic vesicle. Modulation of the transactivating function of *Six1* by *Shh* signaling would be one of the plausible mechanisms. However, we cannot exclude

Discussion

Establishment of otic vesicle patterning by *Six1*

The inner ear originates from a transient embryonic structure, the otic vesicle. Successive transformations and compartmentalization of the otic vesicle give rise to the entire membranous region of inner ear structures. The fate of cells in the otic vesicle is dependent on the gene expression specific to each compartment of the otic vesicle (Fekete, 1999). For example, *Dlx5*, which is expressed in the dorsal side of the otic vesicle, is required for the formation of the semicircular canals (Acampora et al., 1999; Depew et al., 1999). *Otx1*, which is expressed in the ventral side, is needed for the correct morphogenesis of the cochlea (Acampora et al., 1996). The establishment of such a gene expression profile in the otic vesicle, orchestrated by networks or cascades of transcription factors, is essential for inner ear development. However, the genes involved in these networks and components of the cascades are largely unknown. Our study showed for the first time that *Six1* functions to establish the correct expression pattern of many otic genes and contributes to the formation of the majority of inner ear structures. Altered expression pattern of many otic genes (Fig. 5) results in the loss of specifications of the ventral region of the otic vesicle, with resultant expansion of the dorsally specified domains at E9.5-10.5, and consequently in the absence of the cochlea and most of the vestibule, together with dysgenesis of residual region of semicircular canals and enlargement of the endolymphatic sac in *Six1*-deficient neonates (Fig. 2). The ventral expression of *Six1* in the otic vesicle at E9.5-10.5 suggests that *Six1* activates the expression of *Otx1*, *Otx2*, *Lfng* and *Fgf3* and represses the expression of *Dlx5*, *Hmx3*, *Dach1* and *Dach2* (Fig. 8). Although it is unknown whether these genes are regulated

independent actions of *Six1* and components of *Shh* signaling cascades in the otic vesicle. For example, expression of *Pax2* in the medialventral otic vesicle is maintained in *Six1*-deficient mice (Fig. 5S,T), but is downregulated in *Shh*-deficient mice (Riccomagno et al., 2002). To determine whether *Six1* and *Shh* interact genetically, it would be important to examine the phenotypes of the *Six1/Shh* double mutant.

Roles of *Six1* in Pax-Six-Eya-Dach gene network

Six genes function as components of the Pax-Six-Eya-Dach gene network in organ development. In the ventral otic vesicle, *Six1* is co-expressed with *Pax2*, *Pax8*, *Six4* and *Eya1* to control inner ear development. Outside the otic vesicles, various combinations of Pax, Six, Eya and Dach genes are co-expressed in the primordia of the organs affected in *Six1*-deficient mice: the olfactory placode (*Pax6*, *Six1*, *Six2*, *Six3*, *Six4*, *Six6*, *Eya1*, *Eya2*, *Eya4*); the thymus (*Pax9*, *Six1*, *Six4*, *Eya1*); the metanephros (*Pax2*, *Pax8*, *Six1*, *Six2*, *Six4*, *Eya1*); and the somite/myotome (*Pax3*, *Six1*, *Six4*, *Eya1*, *Eya2*, *Eya4*, *Dach1*). *Six1* plays important roles in the development of these organs, probably through the control of patterning and/or cell proliferation, as observed in the otic vesicle. Notably, Dach genes are not co-expressed with Six and Eya genes in the ventral otic vesicle, nose or kidney (Figs 4, 5, data not shown). Furthermore, Dach expression domains were expanded ventrally in the *Six1*-deficient otic vesicle, indicating that *Six1* represses the expression of Dach genes in the ventral otic vesicle. Likewise, augmentation of Dach expression was observed in the nasal pit of *Six1*-deficient embryos (data not shown), indicating that expression of the Dach gene is repressed by *Six1* also in the nasal pit. These findings are in contrast to *Drosophila* compound eye formation and chick myogenesis. In both those cases, Pax, Six and Eya are co-expressed with Dach, cooperatively to execute the developmental programs. Thus, the Pax-Six-Eya gene network lacking Dach may demarcate the two placode-derived sensory organs, the inner ear and the nose, and the kidney from other organs such as the eye and the skeletal muscles. In addition, hierarchy among Pax, Six, Eya and Dach genes in the otic vesicle has been revealed in this study. That is, the expression patterns and levels of *Eya1* and *Pax2* were not affected but expression domains of *Dach1* and *Dach2* were expanded ventrally in the *Six1*-deficient otic vesicle (Fig. 5). Conversely, *Six1* expression is lost but *Pax2* expression is not disturbed in the *Eya1*-deficient otic vesicle (Xu et al., 1999). Thus, in the otic vesicle, expression of *Eya1* and *Pax2* is independent of *Six1*, expression of *Six1* depends on *Eya1*, and *Six1* controls *Dach1* and *Dach2* expression. In the myotome, *Six4* expression is not dependent on *Six1*, as observed in the otic vesicle (Laclef et al., 2003a), but *Pax2* expression is dependent on *Six1* in metanephric mesenchyme (Xu et al., 2003). The similarities among these organ primordia in the context of the Pax-Six-Eya(-Dach) network and the diversity in selecting members from respective gene hierarchies among them raise interesting issues regarding the ontogeny of these organs during evolution.

In conclusion, our study identified the essential role of *Six1* in the regulation of otic vesicle patterning. Together with mice homozygous for other Pax, Six, Eya and Dach genes, *Six1*-deficient mice should allow a comprehensive understanding of the roles of the Pax-Six-Eya-Dach gene network in various organogeneses.

We thank Chin Chiang for providing *Shh*-deficient mice; Yoko Watanabe, Miwa Nakamura and Sachiko Nozawa for technical assistance; Makoto Yamakado, Kuniko Shimazaki and Heide Ford for technical advice; and Makoto Kobayashi and Shigeru Sato for critical reading of the manuscript. We thank Shinichi Aizawa, David Wilkinson, Douglas Epstein, Takashi Momoi, Jun Motoyama, Doris K. Wu, Ryuichi Nishinakamura, Hiroshi Shibuya, Akira Murakami, Naoto Ueno, Stefan Krauss, Graeme Mardon, Peter Gruss and Thomas Lufkin for the plasmids for probes used in this work. We also thank Pascal Maire for sharing the information about *Six1* gene organization. This work was supported by grants from the Ministry of Education, Culture, Sports, Science and Technology of Japan and from the Ministry of Health, Labour and Welfare of Japan.

References

- Acampora, D., Mazan, S., Avantaggiato, V., Barone, P., Tuorto, F., Lallemand, Y., Brulet, P. and Simeone, A. (1996). Epilepsy and brain abnormalities in mice lacking the *Otx1* gene. *Nat. Genet.* **14**, 218-222.
- Acampora, D., Merlo, G. R., Paleari, L., Zerega, B., Postiglione, M. P., Mantero, S., Bober, E., Barbieri, O., Simeone, A. and Levi, G. (1999). Craniofacial, vestibular and bone defects in mice lacking the *Distal-less*-related gene *Dlx5*. *Development* **126**, 3795-3809.
- Bissonnette, J. P. and Fekete, D. M. (1996). Standard atlas of the gross anatomy of the developing inner ear of the chicken. *J. Comp. Neurol.* **368**, 620-630.
- Carl, M., Loosli, F. and Wittbrodt, J. (2002). *Six3* inactivation reveals its essential role for the formation and patterning of the vertebrate eye. *Development* **129**, 4057-4063.
- Caubit, X., Thangarajah, R., Theil, T., Wirth, J., Nothwang, H.-G., Ruther, U. and Krauss, S. (1999). Mouse *Dac*, a novel nuclear factor with homology to *Drosophila* *dachshund* shows a dynamic expression in the neural crest, the eye, the neocortex, and the limb bud. *Dev. Dyn.* **214**, 66-80.
- Chen, R., Amoui, M., Zhang, Z. and Mardon, G. (1997). *Dachshund* and eyes absent proteins form a complex and function synergistically to induce ectopic eye development in *Drosophila*. *Cell* **91**, 893-903.
- Chiang, C., Litingtung, Y., Lee, E., Young, K. E., Corden, J. L., Westphal, H. and Beachy, P. A. (1996). Cyclopia and defective axial patterning in mice lacking *Sonic hedgehog* gene function. *Nature* **383**, 407-413.
- Czerny, T., Halder, G., Kloter, U., Souabni, A., Gehring, W. J. and Busslinger, M. (1999). Twin of *eyeless*, a second *Pax-6* gene of *Drosophila*, acts upstream of *eyeless* in the control of eye development. *Mol. Cell* **3**, 297-307.
- Davis, R. J., Shen, W., Sandler, Y. I., Heanue, T. A. and Mardon, G. (2001). Characterization of mouse *Dach2*, a homologue of *Drosophila* *dachshund*. *Mech. Dev.* **102**, 169-179.
- Depew, M. J., Liu, J. K., Long, J. E., Presley, R., Meneses, J. J., Pedersen, R. A. and Rubenstein, J. L. (1999). *Dlx5* regulates regional development of the branchial arches and sensory capsules. *Development* **126**, 3831-3846.
- Favor, J., Sandulache, R., Neuhauser-Klaus, A., Pretsch, W., Chatterjee, B., Senft, E., Wurst, W., Blanquet, V., Grimes, P., Sporle, R. et al. (1996). The mouse *Pax2*^{1Neu} mutation is identical to a human *PAX2* mutation in a family with renal-coloboma syndrome and results in developmental defects of the brain, ear, eye, and kidney. *Proc. Natl. Acad. Sci. USA* **93**, 13870-13875.
- Fekete, D. M. (1999). Development of the vertebrate ear: insights from knockouts and mutants. *Trends Neurosci.* **22**, 263-269.
- Ford, H. L., Kabingu, E. N., Bump, E. A., Mutter, G. L. and Pardee, A. B. (1998). Abrogation of the G₂ cell cycle checkpoint associated with overexpression of *HSIX1*: a possible mechanism of breast carcinogenesis. *Proc. Natl. Acad. Sci. USA* **95**, 12608-12613.
- Glaser, T., Walton, D. S. and Maas, R. L. (1992). Genomic structure, evolutionary conservation and aniridia mutations in the human *PAX6* gene. *Nat. Genet.* **2**, 232-239.
- Goodrich, L. V., Johnson, R. L., Milenkovic, L., McMahon, J. A. and Scott, M. P. (1996). Conservation of the hedgehog/patched signaling pathway from flies to mice: induction of a mouse patched gene by *Hedgehog*. *Genes Dev.* **10**, 301-312.
- Halder, G., Callaerts, P., Flister, S., Walldorf, U., Kloter, U. and Gehring, W. J. (1998). *Eyeless* initiates the expression of both *sine oculis* and *eyes*

- absent during *Drosophila* compound eye development. *Development* **125**, 2181-2191.
- Heanue, T. A., Reshef, R., Davis, R. J., Mardon, G., Oliver, G., Tomarev, S., Lassar, A. B. and Tabin, C. J. (1999). Synergistic regulation of vertebrate muscle development by *Dach2*, *Eya2*, and *Six1*, homologs of genes required for *Drosophila* eye formation. *Genes Dev.* **13**, 3231-3243.
- Hill, R. E., Favor, J., Hogan, B. L., Ton, C. C., Saunders, G. F., Hanson, I. M., Prosser, J., Jordan, T., Hastie, N. D. and van Heyningen, V. (1991). Mouse small eye results from mutations in a paired-like homeobox-containing gene. *Nature* **354**, 522-525.
- Horai, R., Asano, M., Sudo, K., Kanuka, H., Suzuki, M., Nishihara, M., Takahashi, M. and Iwakura, Y. (1998). Production of mice deficient in genes for interleukin (IL)-1 α , IL-1 β , IL-1 α/β , and IL-1 receptor antagonist shows that IL-1 β is crucial in turpentine-induced fever development and glucocorticoid secretion. *J. Exp. Med.* **187**, 1463-1475.
- Hui, C. C., Slusarski, D., Platt, K. A., Holmgren, R. and Joyner, A. L. (1994). Expression of three mouse homologs of the *Drosophila* segment polarity gene *cubitus interruptus*, *Gli*, *Gli-2*, and *Gli-3*, in ectoderm- and mesoderm-derived tissues suggests multiple roles during postimplantation development. *Dev. Biol.* **162**, 402-413.
- Kardon, G., Heanue, T. A. and Tabin, C. J. (2002). Pax3 and *Dach2* positive regulation in the developing somite. *Dev. Dyn.* **224**, 350-355.
- Kawakami, K., Ohto, H., Ikeda, K. and Roeder, R. G. (1996). Structure, function and expression of a murine homeobox protein AREC3, a homologue of *Drosophila sine oculis* gene product, and implication in development. *Nucleic Acids Res.* **24**, 303-310.
- Kawakami, K., Sato, S., Ozaki, H. and Ikeda, K. (2000). Six family genes-structure and function as transcription factors and their roles in development. *Bioessays* **22**, 616-626.
- Kobayashi, M., Toyama, R., Takeda, H., Dawid, I. B. and Kawakami, K. (1998). Overexpression of the forebrain-specific homeobox gene *six3* induces rostral forebrain enlargement in zebrafish. *Development* **125**, 2973-2982.
- Kuhn, R., Rajewsky, K. and Muller, W. (1991). Generation and analysis of interleukin-4 deficient mice. *Science* **254**, 707-710.
- Laclef, C., Hamard, G., Demignon, J., Souil, E., Houbbron, C. and Maire, P. (2003a). Altered myogenesis in *Six1*-deficient mice. *Development* **130**, 2239-2252.
- Laclef, C., Souil, E., Demignon, J. and Maire, P. (2003b). Thymus, kidney and craniofacial abnormalities in *Six1* deficient mice. *Mech. Dev.* **120**, 669-679.
- Lagutin, O., Zhu, C. C., Furuta, Y., Rowitch, D. H., McMahon, A. P. and Oliver, G. (2001). *Six3* promotes the formation of ectopic optic vesicle-like structures in mouse embryos. *Dev. Dyn.* **221**, 342-349.
- Lagutin, O. V., Zhu, C. C., Kobayashi, D., Topczewski, J., Shimamura, K., Puelles, L., Russell, H. R., McKinnon, P. J., Solnica-Krezel, L. and Oliver, G. (2003). *Six3* repression of Wnt signaling in the anterior neuroectoderm is essential for vertebrate forebrain development. *Genes Dev.* **17**, 368-379.
- Li, X., Perissi, V., Liu, F., Rose, D. W. and Rosenfeld, M. G. (2002). Tissue-specific regulation of retinal and pituitary precursor cell proliferation. *Science* **297**, 1180-1183.
- Loosli, F., Winkler, S. and Wittbrodt, J. (1999). *Six3* overexpression initiates the formation of ectopic retina. *Genes Dev.* **13**, 649-654.
- Mansour, S. L., Goddard, J. M. and Capecchi, M. R. (1993). Mice homozygous for a targeted disruption of the proto-oncogene *int-2* have developmental defects in the tail and inner ear. *Development* **117**, 13-28.
- Matsuo, I., Kuratani, S., Kimura, C., Takeda, N. and Aizawa, S. (1995). Mouse *Otx2* functions in the formation and patterning of rostral head. *Genes Dev.* **9**, 2646-2658.
- Miyama, K., Yamada, G., Yamamoto, T. S., Takagi, C., Miyado, K., Sakai, M., Ueno, N. and Shibuya, H. (1999). A BMP-inducible gene, *Dlx5*, regulates osteoblast differentiation and mesoderm induction. *Dev. Biol.* **208**, 123-133.
- Morsli, H., Choo, D., Ryan, A., Johnson, R. and Wu, D. K. (1998). Development of the mouse inner ear and origin of its sensory organs. *J. Neurosci.* **18**, 3327-3335.
- Morsli, H., Tuorto, F., Choo, D., Postiglione, M. P., Simeone, A. and Wu, D. K. (1999). *Otx1* and *Otx2* activities are required for the normal development of the mouse inner ear. *Development* **126**, 2335-2343.
- Niimi, T., Seimiya, M., Kloter, U., Flister, S. and Gehring, W. J. (1999). Direct regulatory interaction of the eyeless protein with an eye-specific enhancer in the *sine oculis* gene during eye induction in *Drosophila*. *Development* **126**, 2253-2260.
- Nishinakamura, R., Matsumoto, Y., Nakao, K., Nakamura, K., Sato, A., Copeland, N. G., Gilbert, D. J., Jenkins, N. A., Scully, S., Lacey, D. L. et al. (2001) Murine homolog of *SALL1* is essential for ureteric bud invasion in kidney development. *Development* **128**, 3105-3115.
- Ohto, H., Kamada, S., Tago, K., Tominaga, S. I., Ozaki, H., Sato, S. and Kawakami, K. (1999). Cooperation of *Six* and *Eya* in activation of their target genes through nuclear translocation of *Eya*. *Mol. Cell. Biol.* **19**, 6815-6824.
- Oliver, G., Mailhos, A., Wehr, R., Copeland, N. G., Jenkins, N. A. and Gruss, P. (1995a). *Six3*, a murine homologue of the *sine oculis* gene, demarcates the most anterior border of the developing neural plate and is expressed during eye development. *Development* **121**, 4045-4055.
- Oliver, G., Wehr, R., Jenkins, N. A., Copeland, N. G., Cheyette, B. N. R., Hartenstein, V., Zipursky, S. L. and Gruss, P. (1995b). Homeobox genes and connective tissue patterning. *Development* **121**, 693-705.
- Oliver, G., Loosli, F., Koster, R., Wittbrodt, J. and Gruss, P. (1996). Ectopic lens induction in fish in response to the murine homeobox gene *Six3*. *Mech. Dev.* **60**, 233-239.
- Ozaki, H., Watanabe, Y., Takahashi, K., Kitamura, K., Tanaka, A., Urase, K., Momoi, T., Sudo, K., Sakagami, J., Asano, M. et al. (2001). *Six4*, a putative myogenin gene regulator, is not essential for mouse embryonal development. *Mol. Cell. Biol.* **21**, 3343-3350.
- Pignoni, F., Hu, B., Zavitz, K. H., Xiao, J., Garrity, P. A. and Zipursky, S. L. (1997). The eye-specification proteins *So* and *Eya* form a complex and regulate multiple steps in *Drosophila* eye development. *Cell* **91**, 881-891.
- Riccomagno, M. M., Martinu, L., Mulheisen, M., Wu, D. K. and Epstein, D. J. (2002). Specification of the mammalian cochlea is dependent on Sonic hedgehog. *Genes Dev.* **16**, 2365-2378.
- Ridgeway, A. G. and Skerjanc, I. S. (2001). Pax3 is essential for skeletal myogenesis and the expression of *Six1* and *Eya2*. *J. Biol. Chem.* **276**, 19033-19039.
- Seo, H. C., Curtiss, J., Mlodzik, M. and Fjose, A. (1999). Six class homeobox genes in *Drosophila* belong to three distinct families and are involved in head development. *Mech. Dev.* **83**, 127-139.
- Spitz, F., Demignon, J., Porteu, A., Kahn, A., Concordet, J. P., Daegelen, D. and Maire, P. (1998). Expression of myogenin during embryogenesis is controlled by *Six/sine oculis* homeoproteins through a conserved MEF3 binding site. *Proc. Natl. Acad. Sci. USA* **95**, 14220-14225.
- Ton, C. C., Hirvonen, H., Miwa, H., Weil, M. M., Monaghan, P., Jordan, T., van Heyningen, V., Hastie, N. D., Meijers-Heijboer, H., Drechsler, M. et al. (1991). Positional cloning and characterization of a paired box- and homeobox-containing gene from the aniridia region. *Cell* **67**, 1059-1074.
- Torres, M., Gomez-Pardo, E. and Gruss, P. (1996). Pax2 contributes to inner ear patterning and optic nerve trajectory. *Development* **122**, 3381-3391.
- Toy, J., Yang, J. M., Leppert, G. S. and Sundin, O. H. (1998). The *Otx2* homeobox gene is expressed in early precursors of the eye and activates retina-specific genes. *Proc. Natl. Acad. Sci. USA* **95**, 10643-10648.
- Urase, K., Mukasa, T., Igarashi, H., Ishii, Y., Yasugi, S., Momoi, M. Y. and Momoi, T. (1996). Spatial expression of Sonic hedgehog in the lung epithelium during branching morphogenesis. *Biochem. Biophys. Res. Commun.* **225**, 161-166.
- Wallin, J., Wiltling, J., Koseki, H., Fritsch, R., Christ, B. and Balling, R. (1994). The role of Pax-1 in axial skeleton development. *Development* **120**, 1109-1121.
- Wallis, D. E., Roessler, E., Hehr, U., Nanni, L., Wiltshire, T., Richieri-Costa, A., Gillesen-Kaesbach, G., Zackai, E. H., Rommens, J. and Muenke, M. (1999). Mutations in the homeodomain of the human *SIX3* gene cause holoprosencephaly. *Nat. Genet.* **22**, 196-198.
- Walther, C. and Gruss, P. (1991). Pax-6, a murine paired box gene, is expressed in the developing CNS. *Development* **113**, 1435-1449.
- Wang, W., Van De Water, T. and Lufkin, T. (1998). Inner ear and maternal reproductive defects in mice lacking the *Hmx3* homeobox gene. *Development* **125**, 621-634.
- Wang, W., Chan, E. K., Baron, S., Van De Water, T. and Lufkin, T. (2001). *Hmx2* homeobox gene control of murine vestibular morphogenesis. *Development* **128**, 5017-5029.
- Wilkinson, D. G., Peters, G., Dickson, C. and McMahon, A. P. (1988). Expression of the FGF-related proto-oncogene *int-2* during gastrulation and neurulation in the mouse. *EMBO J.* **7**, 691-695.
- Xu, P.-X., Woo, I., Her, H., Beier, D. R. and Maas, R. L. (1997). Mouse *Eya* homologues of the *Drosophila* eyes absent gene require Pax6 for expression in lens and nasal placode. *Development* **124**, 219-231.
- Xu, P.-X., Adams, J., Peters, H., Brown, M. C., Heaney, S. and Maas, R.

- (1999). Eya1-deficient mice lack ears and kidneys and show abnormal apoptosis of organ primordia. *Nat. Genet.* **23**, 113-117.
- Xu, P.-X., Zheng, W., Laclef, C., Maire, P., Maas, R. L., Peters, H. and Xu, X.** (2002). Eya1 is required for the morphogenesis of mammalian thymus, parathyroid and thyroid. *Development* **129**, 3033-3044.
- Xu, P.-X., Zheng, W., Huang, L., Maire, P., Laclef, C. and Silvius, D.** (2003). Six1 is required for the early organogenesis of mammalian kidney. *Development* **130**, 3085-3094.
- Xu, Q. and Wilkinson, D. G.** (1998). In situ hybridization of mRNA with hapten labelled probes. In *In Situ Hybridization: a Practical Approach* (ed. D. G. Wilkinson), pp. 87-106. London: Oxford University Press.
- Yagi, T., Nada, S., Watanabe, N., Tamemoto, H., Kohmura, N., Ikawa, Y. and Aizawa, S.** (1993). A novel negative selection for homologous recombinants using diphtheria toxin A fragment gene. *Anal. Biochem.* **214**, 77-86.
- Zimmerman, J. E., Bui, Q. T., Liu, H. and Bonini, N. M.** (2000). Molecular genetic analysis of *Drosophila* eyes absent mutants reveals an eye enhancer element. *Genetics* **154**, 237-246.